Research Article

Iryna I. Grynyuk, Olga M. Vasyliuk, Svitlana V. Prylutska, Nataliia Yu. Strutynska*, Oksana V. Livitska, Mykola S. Slobodyanik

Influence of nanoscale-modified apatite-type calcium phosphates on the biofilm formation by pathogenic microorganisms

https://doi.org/10.1515/chem-2021-0199
received November 13, 2020; accepted January 6, 2021

Abstract: Nanoparticles (25–50 nm) of chemically modified calcium phosphates $Ca_{10-x-y}M^{II}_xNa_y(PO_4)_{6-z}(CO_3)_z(OH)_2$ (M^{II} – Cu^{2+}, Zn^{2+}) were synthesized via a wet precipitation method at room temperature. The Fourier-transform infrared spectroscopy data confirmed the partial substitution of $PO_4^{3-} \rightarrow CO_3^{2-}$ (B-type) in apatite-type structure. The influence of prepared phosphates on biofilm formation by pathogenic microorganisms was investigated. It was found that the samples Na^+, CO_3^{2-}-hydroxyapatite (HAP) and Na^+, Zn^{2+}, CO_3^{2-}-HAP (5–20 mM) had the highest inhibitory effect on biofilm formation by *Staphylococcus aureus* strains. The sample Na^+, CO_3^{2-}-HAP had the slight influence on the formation of the biofilm by *Pseudomonas aeruginosa*, while for the samples Na^+, Cu^{2+}, CO_3^{2-}-HAP and Na^+, Zn^{2+}, CO_3^{2-}-HAP such an effect was not detected. According to transmission electron microscopy data, a correlation between the activity of synthesized apatite-related modified calcium phosphates in the processes of biofilm formation and their ability to adhere to the surface of bacterial cells was established. The prepared samples can be used for the design of effective materials with antibacterial activity for medicine.

Keywords: apatite, nanoparticles, biofilm formation, *Staphylococcus aureus*, *Pseudomonas aeruginosa*

1 Introduction

At present, apatite-type calcium phosphate ($Ca_{10}(PO_4)_6(OH)_2$), hydroxyapatite [HAP]) and its chemically modified analogues owing to its biocompatibility, bioactivity and similarity with bone tissue are widely used in medicine, in particular, orthopedics and dentistry for bone restoration and coating of orthopedic and dental implants, for oral care, for remineralization of carious lesions of enamel and protection of teeth from caries [1–4]. The surface of these materials due to their physicochemical properties modulates enhanced adhesion of osteoblasts, increases the strength of adhesion of implants to bone tissue, but, unfortunately, this feature can also promote bacterial adhesion. Bacterial infections associated with implants and medical devices are a serious clinical problem. Such infections are difficult to treat with antibacterial agents because the bacteria that cause the infection can form biofilms on the surface of the implant [5–8].

Bacterial biofilms are complex structures of microbial cells, which are embedded in an extracellular matrix and attached to biotic or abiotic surfaces. The biofilm matrix consists of exopolysaccharides, proteins, teichoic acids, lipids and DNAs [9,10]. Biofilms can protect planktonic bacteria from the immune system of the host by disrupting the activation of complement system and phagocytes, and increasing pathogenic bacteria resistance to antibiotics around 1,000-fold [11–14].

Three-quarters of all biofilm-related infections on medical devices are formed by *Staphylococcus aureus*, *Staphylococcus epidermidis* or *Pseudomonas aeruginosa* [15]. It should be noted that different factors influence the formation of biofilms such as the type and surface on characteristics of biomaterial as well as the type of bacteria and their concentration, temperature, pH and nutrients. Hence, creation of materials with special characteristics, which reduce bacterial adhesion and inhibit the formation of bacterial biofilms, is very important. Investigation of the influence of chemical and morphological

* **Corresponding author: Nataliia Yu. Strutynska,** Department Chemistry, Taras Shevchenko National University of Kyiv, 64/13, Volodymyrska Str., 01601, Kyiv, Ukraine, e-mail: Strutynska_N@bigmir.net
Iryna I. Grynyuk, Svitlana V. Prylutska, Oksana V. Livitska, Mykola S. Slobodyanik: Department Chemistry, Taras Shevchenko National University of Kyiv, 64/13, Volodymyrska Str., 01601, Kyiv, Ukraine
Olga M. Vasyliuk: Department of Physiology of Industrial Microorganisms, Zabolotny Institute of Microbiology and Virology, National Academy of Science of Ukraine, 154, Zabolotnogo str, 03143, Kyiv, Ukraine

modifications of apatite-related calcium phosphate on the biofilm formation by the most common strains is important for the design of effective biomaterials. This will further avoid the development of pathological processes while using materials based on apatite.

A lot of literature data are devoted to the study of the antimicrobial properties of HAPs doped with different cations [16–26]. It was shown that Ag-HAP exhibits strong antibacterial activity [17,18]. The silver ions are slowly released from the interior of the HAP, which discloses its bactericidal activity throughout the material surrounding it [19]. HAPs doped with Cu^{2+} have inhibitory effect on the growth of *Escherichia coli* [20]. The antibacterial behavior of Zn^{2+}-doped HAP has also been studied [21,22], while its nanorods are reported to have improved performance against oral cavity bacteria [23]. A significant decrease in the number of viable *Staphylococcus aureus* bacteria was found after in contact with Zn-doped HAP [24]. The incorporation of Mg^{2+}, Ni^{2+} and SiO_4 ions into the HAP structure also showed *in vitro* antibacterial activity against *Escherichia coli* and *Pseudomonas aeruginosa* [25,26]. Predoi et al. showed that Ce-HAP suspensions had a biocide effect against *Escherichia coli* and *Candida albicans* microbial strains [27]. Thus, one of the approaches to enhance the antimicrobial properties of apatite-based materials is modification of initial matrix by cations with antibacterial properties, in particular silver (Ag^{+}), zinc (Zn^{2+}) or copper (Cu^{2+}). Another promising approach is the fabrication of HAP composite with antibacterial properties such as nano HAP-ZnO composites [28] and HAP-Ag [29].

The main goal of the present work was to investigate the influence of chemically modified apatite-related calcium phosphate on the biofilm formation of *Staphylococcus aureus* and *Pseudomonas aeruginosa* strains. These cultures are the most important pathogens causing bone and joint infections. The apatite-related calcium phosphates which contained different dopants (Na^{+}, CO_3^{2} or Na^{+}, Zn^{2+}, CO_3^{2-} or Na^{+}, Cu^{2+}, CO_3^{2-}) were synthesized and their antibiofilm effect were evaluated. Such investigation is important for the creation of effective materials with antimicrobial activity for medical purposes.

2 Materials and methods

2.1 Preparation of chemically modified calcium phosphates

Chemically modified apatite-related calcium phosphates (Na^{+}, CO_3^{2-}-HAP, Na^{+}, Zn^{2+}, CO_3^{2-}-HAP and Na^{+}, Cu^{2+}, CO_3^{2-}-HAP) were synthesized via a wet precipitation method at molar ratios Ca/P = 1.67, PO_4^{3-}/CO_3^{2-} = 1 and M^{II}:Ca = 1:50 (M^{II} = Cu^{2+}, Zn^{2+}) at the temperature of 25°C. Compounds $Ca(NO_3)_2{\cdot}4H_2O$, $Zn(NO_3)_2{\cdot}6H_2O$, $Cu(NO_3)_2{\cdot}6H_2O$, Na_2CO_3 and Na_3PO_4 were used as starting materials. Nitrate mixture ($Ca(NO_3)_2{\cdot}4H_2O$ and $M^{II}(NO_3)_2{\cdot}6H_2O$) was dissolved in water and added to the solution containing sodium phosphate and carbonate with magnetic stirring (pH = 14). The concentration of all used solutions was 0.1 M. The obtained precipitate was stirred for 15 min, and then solid was filtered and washed with distilled water to eliminate any residual salts. The powders were dried at 100°C for 80 h. The prepared Na^{+}, CO_3^{2-}-HAP was also annealed at a temperature of 700°C for 1 h. Drying oven SingleDISPLAY and muffle furnace SNOL-7.2/1100 (TermoPro-601 temperature controller) were used for drying and annealing of samples.

2.2 Characterization of prepared calcium phosphates

The phase composition of prepared samples was determined by powder X-ray diffraction (XRD) method. Diffractograms were recorded using Shimadzu XRD-6000 diffractometer with Cu-Kα radiation (λ = 1.54178 Å, 2θ = 5–90°, step size = 0.01°).

The presence of different anion types in the synthesized phase was detected by Fourier-transform infrared spectroscopy (FTIR). PerkinElmer Spectrum BX spectrometer was used in the frequency range of 400–4,000 cm^{-1} at 1 cm^{-1} resolution for samples pressed in KBr pellets.

Surface characteristics (shape, size and elemental composition) of samples were investigated by scanning electron microscopy (SEM; FEI Quanta 400 ESEM instrument) with EDX analizator (Genesis 4000 instrument).

The amount of calcium, sodium, zinc, copper and phosphorus was additionally defined by atomic absorption spectroscopy (Thermo Electron M-Series instrument) after dissolution of the particles in hydrochloric acid, while the amount of carbon was measured using CHN elemental analysis (Elementar Analysensysteme).

2.3 Antibacterial activity

The effect of synthesized modified calcium phosphates on the biofilm formation by pathogenic microorganisms was investigated according to the study by Rode et al. [30] with some modifications. All prepared samples were sterilized before use by autoclaving for 30 min at 112°C

(0.75 atm). The reference cultures *Staphylococcus aureus* ATCC 25923 and *Pseudomonas aeruginosa* ATCC 9027 were used for the investigation of antibiofilm effect of the synthesized samples. These cultures are medically relevant bacterial strains and the most important pathogens causing bone and joint infections. *S. aureus* is a gram-positive facultative anaerobic cocci and *P. aeruginosa* is a gram-negative facultative anaerobic rod. *S. aureus* and *P. aeruginosa* are highly virulent multidrug-resistant strains that establish dangerous infections and in many instances are very difficult to be treated with the existing medicines [31–33]. Almost 70% biofilm-related infections on medical devices are formed by *S. aureus* or *P. aeruginosa* [15,34].

Suspensions of 24 h bacterial culture such as *S. aureus* and *P. aeruginosa* strains were grown on tryptone soy broth at 37°C. Opportunistic strains were grown at 37°C for 18 h on liquid culture medium – tryptone soy broth (HiMedia).

Different amounts (5, 10 and 20 mM) of the synthesized samples were added to 96-well plates with sterile nutrient medium. Then the inoculum (10^7 CFU/mL) was added. All systems were incubated at 37°C for 24 h.

The optical density was measured as absorbance at λ = 630 nm using Reader Multiskan FC (Thermo Fisher Scientific, USA). The culture fluid was poured off, and the wells were washed three times with sterile phosphate-buffered saline (PBS) buffer. The plates were air dried for 30 min and then stained with 0.1% solution of crystalline violet (Sigma, USA). The dye was poured off after 20 min of exposure at room temperature and washed five times with PBS buffer. The plates were air dried for 30 min at room temperature and 0.1 mL of 95% ethanol was added to the wells. After 30 min, the optical density was measured as absorbance at 492 nm.

The morphologic characterization of the synthesized samples (10 mM suspension) with opportunistic pathogens 24 h culture was analyzed using a transmission electron microscope JEM-1400 (JEOL, Japan). Investigated suspension of samples with some microorganisms was applied on the surface of a carbon mesh and dried at room temperature.

The statistical analysis of data was performed using the program ≪STATISTICA 7.0≫ (StatSoft, Inc. USA). The post-hoc-test using the criterion of LSD was used for assessing the reliability of quantitative indicators of differences in different strains. The difference was considered significant at $P \leq 0.05$.

Ethical approval: The conducted research is not related to either human or animal use.

3 Results and discussion

According to the XRD data, synthesized samples are poorly crystalline apatite-related calcium phosphates (Figure 1a). Their powder diffractograms contained two wide reflexes in the ranges 2θ = 23–26° and 31–35°, which are characteristic for apatite-related calcium phosphates [35,36]. Samples did not contain the crystalline impurities. Elemental analysis results showed that the prepared calcium phosphates contained Na^+ – 0.2–0.3 wt%, C – 1.16–1.33 wt%, Cu^{2+} – 1.0 wt% or Zn^{2+} – 1.9 wt% (Table 1). FTIR spectra of all synthesized phosphates are similar with respect to intensity and position of vibration bands, and a general view of these spectra is typical for apatite-type calcium phosphates (Figure 1b). Intensive characteristic modes of symmetric and asymmetric stretching vibrations (ν_4, ν_1 and ν_3) of phosphate tetrahedron are observed in the regions of 560–600 cm^{-1} and 1,000–1,100 cm^{-1}. The broad band in the range of 3,200–3,600 cm^{-1} is caused by vibrations of sorbed water and OH group in apatite-type framework. Characteristic modes of CO_3^{2-} groups were found at 870, 1,428 and 1,452 cm^{-1}. Their position indicated the partial substitution of PO_4^{3-} by CO_3^{2-} (B-type) in apatite-type structure [35,36].

SEM data demonstrated that all synthesized samples contained spherical particles with sizes of 25–50 nm, which did not depend on their chemical composition (Figure 2a, c and d).

Taking into account that biofilm formation depends not only on chemical composition of materials but also their surface characteristics, the influence of particle size of apatite-related phase on its biological properties has also been investigated. On this way, sodium-containing phosphate $Ca_{10-x}Na_x(PO_4)_{6-z}(CO_3)_z(OH)_2$ was annealed at 700°C. As shown in ref. [36], such heating resulted in the particle aggregation and crystallite growth (300–500 nm) without changes in phase composition.

Thus, samples of chemically modified calcium phosphates with general composition $Ca_{10-x-y}M^{II}_xNa_y(PO_4)_{6-z}(CO_3)_z(OH)_2$ (M^{II} –Cu^{2+}, Zn^{2+}) and labeled as Na^+, CO_3^{2-}-HAP (particle size of 25–50 nm), Na^+, CO_3^{2-}-HAP (particle size of 300–500 nm), Na^+, Zn^{2+}, CO_3^{2-}-HAP and Na^+, Cu^{2+}, CO_3^{2-}-HAP were synthesized, followed by the investigation of their effect on biofilm formation by opportunistic pathogens *Staphylococcus aureus* and *Pseudomonas aeruginosa*.

Infections associated with the formation of bacterial biofilms on implants are mainly caused by staphylococci. The biofilm of these bacteria on the surface of the implant protects microorganisms from the immune system of the

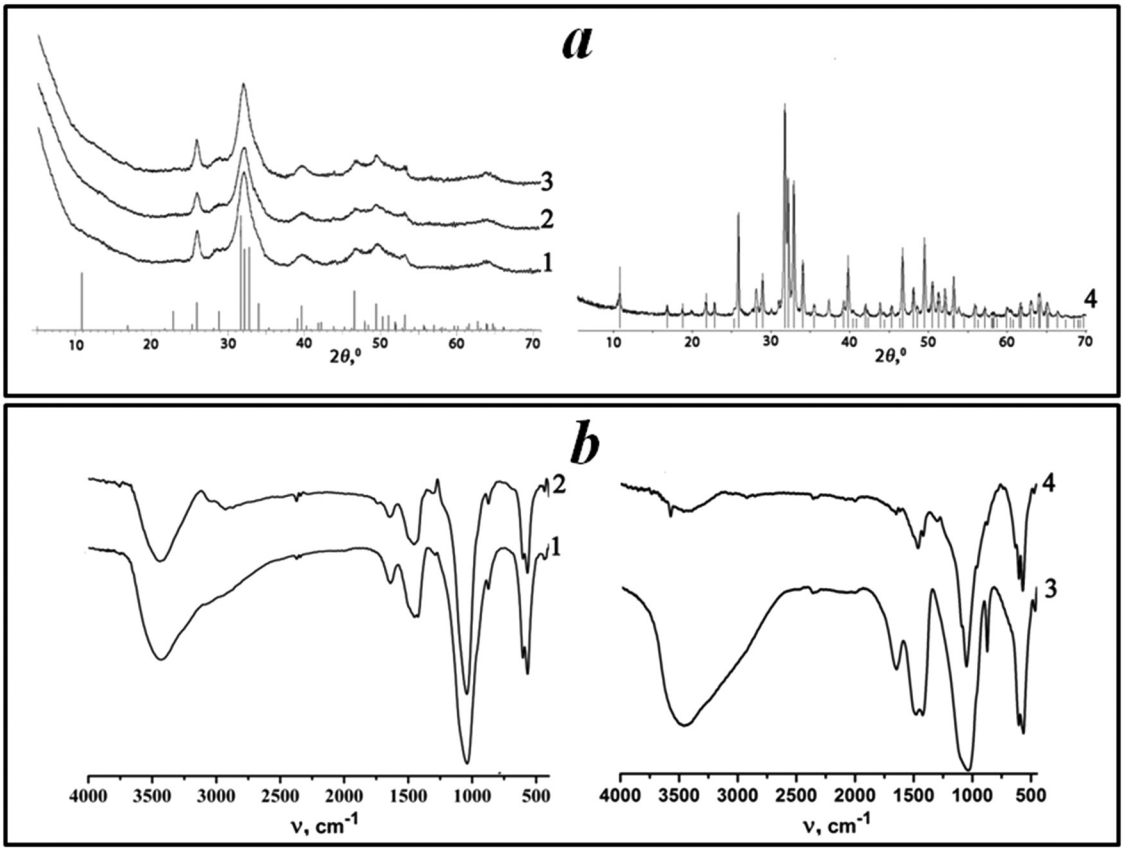

Figure 1: XRD patterns (a) and FTIR spectra (b) of the prepared samples: Na^+, Zn^{2+}, CO_3^{2-}-HAP (curve 1), Na^+, Cu^{2+}, CO_3^{2-}-HAP (curve 2) and Na^+, CO_3^{2-}-HAP (particle sizes of 25–50 nm – curve 3 and 300–500 nm – curve 4) (ICDD, $Ca_{10}(PO_4)_6(OH)_2$ #01-082-1943).

host and also increases their resistance against antibiotics [6,15,37]. Bacterial biofilm formation is a complex multi-stage biological process that involves the adhesion of planktonic bacteria to the surface, proliferation, subsequent accumulation of cell biomass in the form of a multilayer structure containing a polymeric extracellular matrix, maturation and propagation of biofilm fragments [6,7,9,10].

Biofilm formation can be assessed by various methods. One of the standard methods of research on

Table 1: Elemental analysis results for synthesized calcium phosphates

Sample	Weight percent (%)					
	Ca	Na	Cu	Zn	P	C
Na^+, CO_3^{2-}-HAP	37.6	0.3	—	—	18.0	1.33
Na^+, Cu^{2+}, CO_3^{2-}-HAP	35.9	0.2	1.0	—	17.2	1.23
Na^+, Zn^{2+}, CO_3^{2-}-HAP	32.0	0.2	—	1.9	15.9	1.16

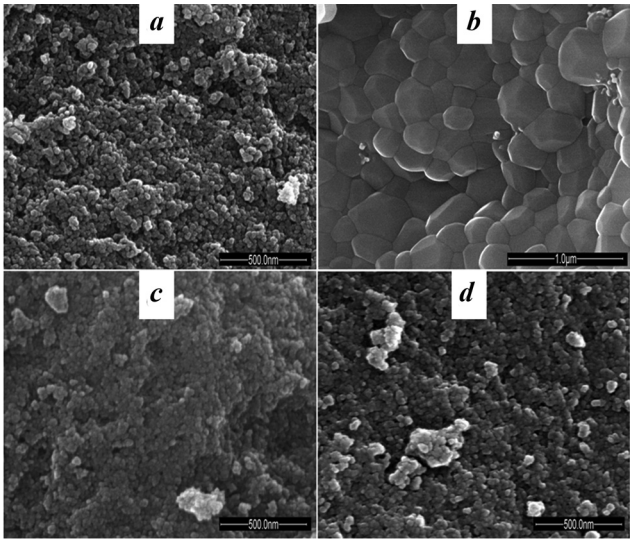

Figure 2: SEM images of the synthesized calcium phosphates: Na^+, CO_3^{2-}-HAP with particle size in the ranges: 25–50 nm (a) and 300–500 nm (b), Na^+, Zn^{2+}, CO_3^{2-}-HAP (c), Na^+, Cu^{2+}, CO_3^{2-}-HAP (d).

the presence of biofilm is crystal violet analysis due to the quantitative determination of the dye bound to bacterial cells on polystyrene. Therefore, the study of the influence of the synthesized samples: Na^+, CO_3^{2-}-HAP (particle size of 25–50 nm), Na^+, CO_3^{2-}-HAP (particle size of 300–500 nm), Na^+, Zn^{2+}, CO_3^{2-}-HAP and Na^+, Cu^{2+}, CO_3^{2-}-HAP on biofilm formation by the *S. aureus* strain was performed by this method for 24 h. It was found that all synthesized samples inhibited the biofilm formation by the *S. aureus* strain (Figure 3). The samples Na^+, CO_3^{2-}-HAP (particles of size 25–50 nm) and Na^+, Zn^{2+}, CO_3^{2-}-HAP had the highest inhibitory effect on the biofilm formation. Thus, increase in amount of sample Na^+, CO_3^{2-}-HAP from 5 to 10 mM and 20 mM led to decrease in the coefficient of formation of the biofilm by the test strain on 55.3, 76.3 and 84.2%, respectively (Figure 3). In particular, for the Na^+, Zn^{2+}, CO_3^{2-}-HAP, the decrease in the biofilm coefficient is slightly higher (63.2, 81.6 and 79.7% for amount of sample 5, 10 and 20 mM, respectively). This result indicates that modification of apatite-type structure by 2 wt% of Zn^{2+} ions leads to an increase in inhibitory effect of phosphate on biofilm formation by the *S. aureus* strain.

It should be noted that antibiofilm-forming activity of Zn-containing apatite to the resistant strains of *Staphylococcus aureus* was previously demonstrated in refs [38,39]. Inhibition of biofilm formation by Zn-doped apatites can be caused by general Zn^{2+} toxicity to bacteria above physiological concentrations but also other biofilm-specific mechanisms of action could be involved. For example, it has been proposed that sublethal Zn^{2+} or Ag^+ concentrations could affect biofilm formation by interfering with quorum sensing [40] or modulate amyloid fibril formation [41]. Other samples Na^+, Cu^{2+}, CO_3^{2-}-HAP and Na^+, CO_3^{2-}-HAP (particles of size 300–500 nm) inhibited biofilm formation to a lesser extent (Figure 3). It should be noted that increase in the particle size of Na^+, CO_3^{2-}-HAP from 25–50 nm to 300–500 nm at concentrations of 5 and 20 mM led to a significant decrease in phosphate activity (Figure 3). However, the effective use of Na^+, Cu^{2+}, CO_3^{2-}-HAP resulted in a slight inhibitory

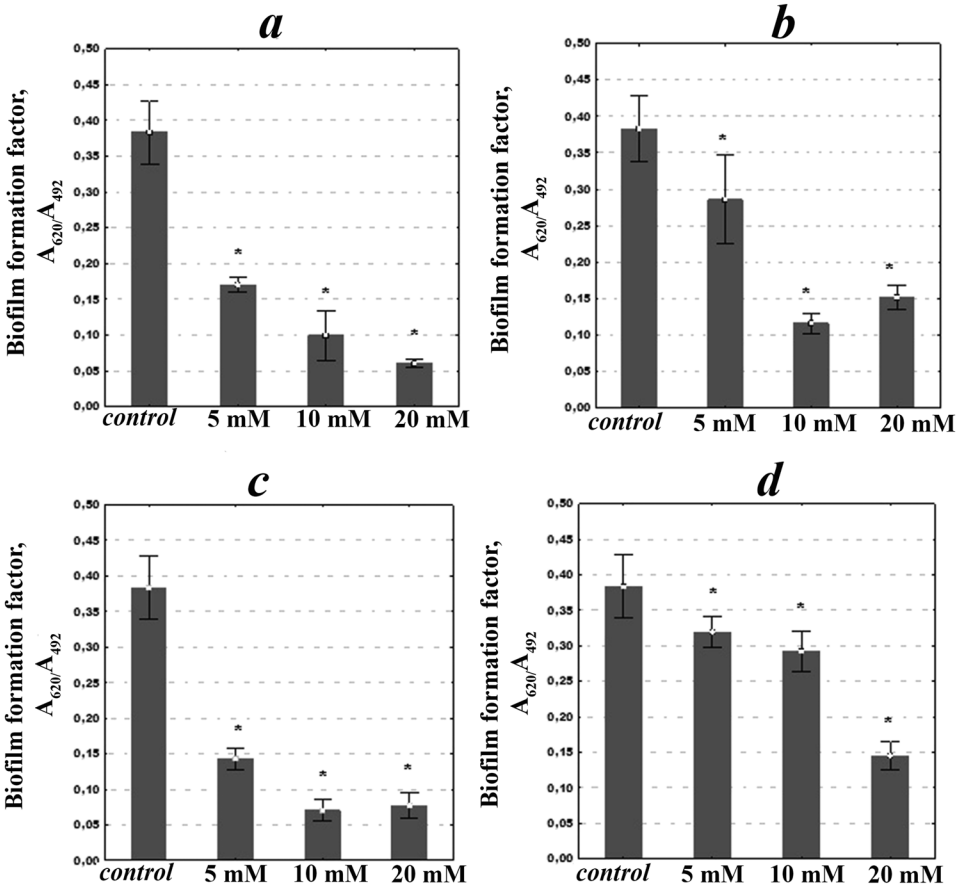

Figure 3: Effect of synthesized apatite-related calcium phosphates on biofilm formation of *S. aureus* strain (M ± m, $n = 4$); *$p < 0.05$ in comparison with control: Na^+, CO_3^{2-}-HAP with particle size in the ranges: 25–50 nm (a) and 300–500 nm (b), Na^+, Zn^{2+}, CO_3^{2-}-HAP (c), Na^+, Cu^{2+}, CO_3^{2-}-HAP (d).

effect on the biofilm formation of *S. aureus*. It is known from the literature data that gram-positive microorganisms, in particular, the *S. aureus* strains have acquired resistance to the toxic effects of copper [16,42].

Analysis of influence of the synthesized samples on the biofilm formation by the *P. aeruginosa* strain showed the lower activity and only for samples that did not contain Cu^{2+} and Zn^{2+} ions (Figure 4). Thus, in the presence of the sample Na^+, CO_3^{2-}-HAP (with particle sizes in the range of 25–50 nm) the biofilm coefficient decreased only on 28, 49.3 and 41.3% at the amounts of phosphate equal to 5, 10 and 20 mM, respectively.

Inhibition of biofilm formation on 50% compared to the control was found for both samples Na^+, CO_3^{2-}-HAP with particle size of 25–50 and 300–500 nm at their amount of 10 mM.

Thus, the obtained results indicate that the activity of the synthesized chemically modified calcium phosphates to the inhibition of biofilm formation by test cultures *S. aureus* and *P. aeruginosa* depends on the size of their nanoparticles and nature of dopants.

The similar results of significant antimicrobial action of modified apatite-type calcium phosphates against gram-positive microorganisms (*S. aureus*) in comparison with gram-negative (*P. aeruginosa*) were previously reported in ref. [43]. Therefore, the decrease in biofilm formation of opportunistic pathogens under the action of synthesized chemically modified calcium phosphates may be associated with a decrease in the number of viable bacteria due to mechanical destruction of bacterial cells on the surface of nanoscale structures. In addition, similar antibacterial effect was also recorded in other nanostructured oxide materials [44,45].

The interaction of synthesized modified calcium phosphates with opportunistic pathogens was investigated by the transmission electron microscopy (TEM) method (Figures 5 and 6).

It was found that the influence of the synthesized samples on biofilm formation by microorganisms correlates with their ability to attach to the surface of bacterial cells. The high adhesion of Na^+, CO_3^{2-}-HAP and Na^+, Zn^{2+}, CO_3^{2-}-HAP samples to *S. aureus* inhibited the biofilm

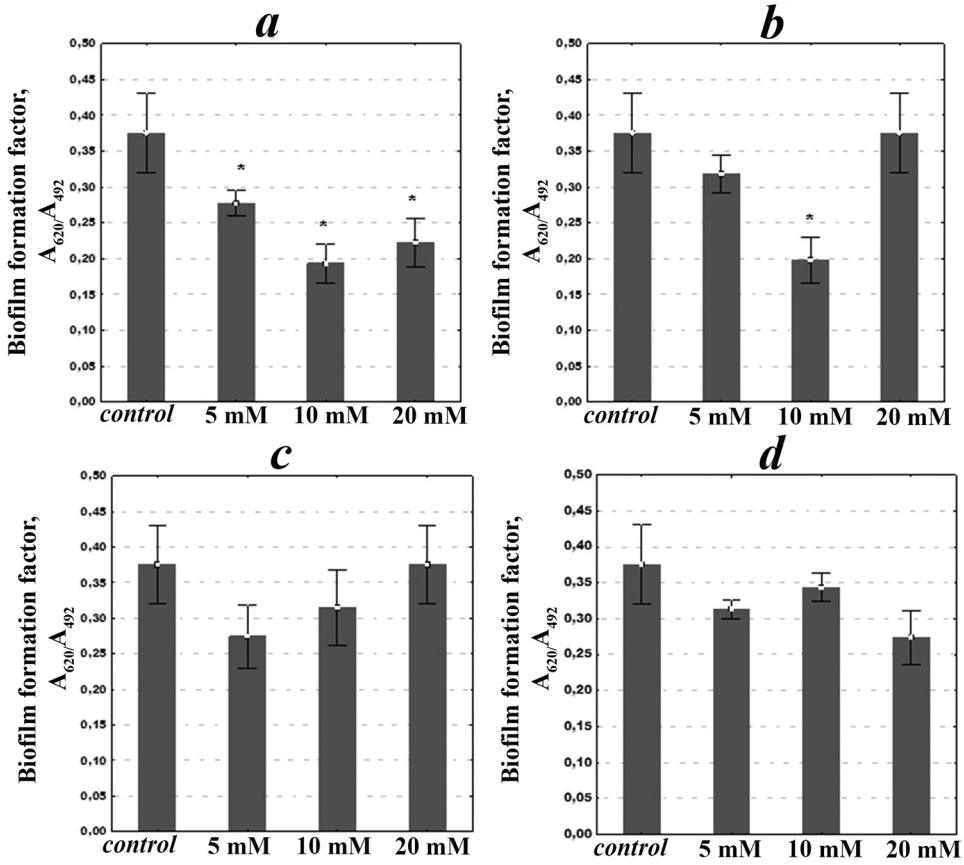

Figure 4: Effect of synthesized calcium phosphates on biofilm formation of *P. aeruginosa* strain (M ± m, $n = 4$); *$p < 0.05$ in comparison with control: Na^+, CO_3^{2-}-HAP with particle sizes in the ranges: 25–50 nm (a) and 300–500 nm (b), Na^+, Zn^{2+}, CO_3^{2-}-HAP (c), Na^+, Cu^{2+}, CO_3^{2-}-HAP (d).

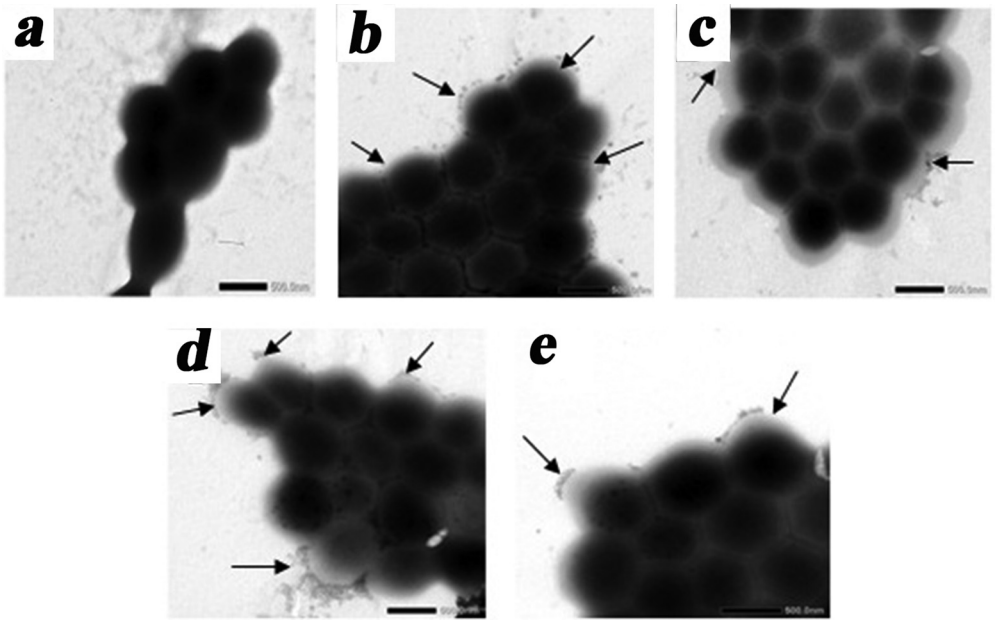

Figure 5: TEM images of *S. aureus* strain in the presence of synthesized phosphates: control *S. aureus* (a), *S. aureus* + Na^+, CO_3^{2-}-HAP with particle size in the ranges: 25–50 nm (b) and 300–500 nm (c), *S. aureus* + Na^+, Zn^{2+}, CO_3^{2-}-HAP (d), *S. aureus* + Na^+, Cu^{2+}, CO_3^{2-}-HAP (e). Scale is 500 nm.

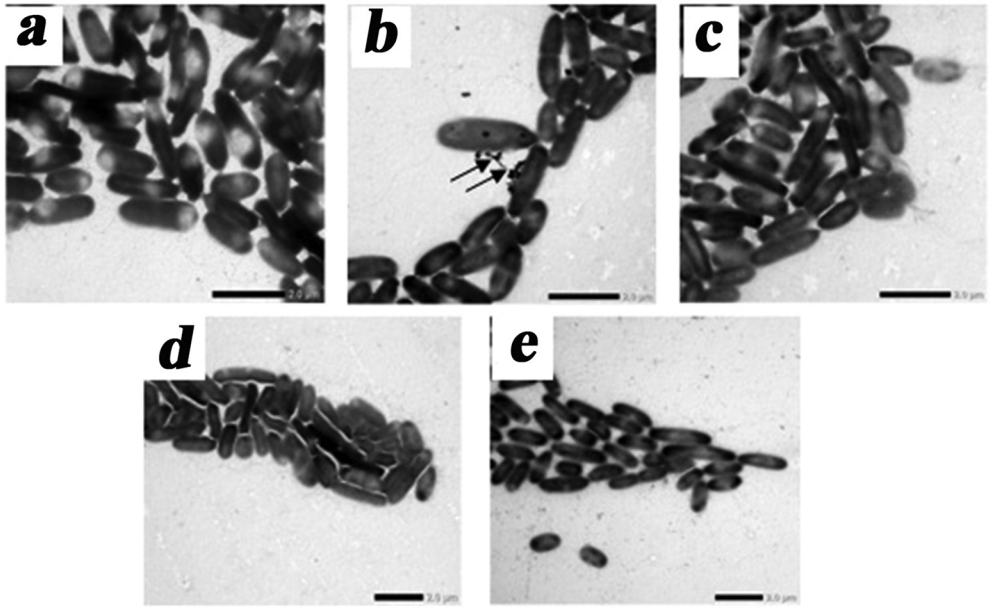

Figure 6: TEM images of *P. aeruginosa* strain in the presence of synthesized phosphates: control *P. aeruginosa* (a), *P. aeruginosa* + Na^+, CO_3^{2-}-HAP with size of particles in the ranges: 25–50 nm (b) and 300–500 nm (c), *P. aeruginosa* + Na^+, Zn^{2+}, CO_3^{2-}-HAP (d), *P. aeruginosa* + Na^+, Cu^{2+}, CO_3^{2-}-HAP (e). Scale is 2.0 µm.

formation (Figure 5). A slight adhesion of gram-negative strain of *P. aeruginosa* to phosphates may explain the low inhibitory activity of sample Na^+, CO_3^{2-}-HAP and its absence for samples Na^+, Cu^{2+}, CO_3^{2-}-HAP and Na^+, Zn^{2+}, CO_3^{2-}-HAP in the biofilm formation (Figure 6).

4 Conclusions

The nanoscale (25–50 nm) particles of chemically modified calcium phosphates for the potential orthopedic application were synthesized by the precipitation method

and their influence on biofilm formation by pathogenic microorganisms was investigated. The prepared apatite-related calcium phosphates $Ca_{10-x-y}M^{II}_xNa_y(PO_4)_{6-z}(CO_3)_z(OH)_2$ (M^{II} – Cu^{2+}, Zn^{2+}) contained 0.2–0.3 wt% – Na^+, 1.16–1.33 wt% – C and 1.0 wt% – Cu^{2+} or 1.9 wt% – Zn^{2+}. According to FTIR data, the partial substitution of phosphate by carbonate groups occurred in apatite-type structure. Differences in the ability of synthesized modified calcium phosphates to inhibit biofilm formation by gram-positive (*S. aureus*) and gram-negative (*P. aeruginosa*) bacteria were found. Our results indicated that all investigated samples had an inhibitory effect on the biofilm formation of *S. aureus*, the highest effect was found for samples Na^+, CO_3^{2-}-HAP and Na^+, Zn^{2+}, CO_3^{2-}-HAP (at the investigated amounts of 5–20 mM). The sample of Na^+, CO_3^{2-}-HAP with particle sizes in the range of 25–50 nm (at the concentration range of 5–20 mM) and 300–500 nm (at the concentration of 10 mM) had the significantly less influence on the formation of the biofilm by *P. aeruginosa*. For samples Na^+, Cu^{2+}, CO_3^{2-}-HAP and Na^+, Zn^{2+}, CO_3^{2-}-HAP, inhibitory effect on biofilm formation by test strain of *P. aeruginosa* was not detected. TEM data showed that the activity of calcium phosphates in the processes of biofilm formation by opportunistic pathogens depended on their ability to adhere to the surface of bacterial cells. The obtained results demonstrated the prospects of using synthesized apatite-related chemically modified calcium phosphates in the development of materials with antimicrobial activity for biomedical purposes.

Funding: This study was supported by the MES of Ukraine (RN 0119U100316).

Author contributions: I. G. – formal analysis; O. V. – investigation; S. P. – validation; N. S. – writing – review and editing; O. L. – investigation; and N. S. – conceptualization.

Conflict of interest: The authors declare no conflict of interest.

Data availability statement: All data generated or analyzed during this study are included in this published article.

References

[1] Balasubramanian S, Gurumurthy B, Balasubramanian A. Biomedical applications of ceramic nanomaterials: a review. Int J Pharm Sci Res. 2017;8(12):4950–9. doi: 10.13040/IJPSR.0975-8232.8(12).4950-59.

[2] Pepla E, Besharat LK, Palaia G, Tenore G, Migliau G. Nano-hydroxyapatite and its applications in preventive, restorative and regenerative dentistry: a review of literature. Ann Stomatol. 2014;5(3):108–14. doi: 10.11138/ads/2014.5.3.108.

[3] Turon P, del Valle LJ, Alemán C, Puiggalí J. Biodegradable and biocompatible systems based on hydroxyapatite nanoparticles. Appl Sci. 2017;7(1):60. doi: 10.3390/app7010060.

[4] Nobre CMG, Pütz N, Hannig M. Adhesion of hydroxyapatite nanoparticles to dental materials under oral conditions. Scanning. 2020;2020:6065739. doi: 10.1155/2020/6065739.

[5] Rimondini L, Fini M, Giardino R. The microbial infection of biomaterials: a challenge for clinicians and researchers. A short review. J Appl Biomater Biomech. 2005;3(1):1–10. doi: 10.1177/228080000500300101.

[6] Arciola CR, Campoccia D, Ehrlich GD, Montanaro L. Biofilm-based implant infections in orthopaedics. Adv Exp Med Biol. 2015;83:29–46. doi: 10.1007/978-3-319-11038-7_2.

[7] Davidson DJ, Spratt, D, Liddle, AD. Implant materials and prosthetic joint infection: the battle with the biofilm. EFORT Open Rev. 2019;4:633–9. doi: 10.1302/2058-5241.4.180095.

[8] Hiltunen AK, Savijoki K, Nyman TA, Miettinen I, Ihalainen P, Peltonen J, et al. Structural and functional dynamics of staphylococcus aureus biofilms and biofilm matrix proteins on different clinical materials. Microorganisms. 2019;7:584. doi: 10.3390/microorganisms7120584.

[9] Jamal M, Ahmad W, Andleeb S, Jalil F, Imran M, Nawaz MA, et al. Bacterial biofilm and associated infections. J Chin Medical Assoc. 2018;81(1):7–11. doi: 10.1016/j.jcma.2017.07.012.

[10] Muhammad MH, Idris AL, Fan X, Guo Y, Yu Y, Jin X, et al. Beyond risk: bacterial biofilms and their regulating approaches. Front Microbiol. 2020;11:928. doi: 10.3389/fmicb.2020.00928.

[11] Penesyan A, Gillings M, Paulsen IT. Antibiotic discovery: combatting bacterial resistance in cells and in biofilm communities. Molecules. 2015;20:5286–98. doi: 10.3390/molecules20045286.

[12] Roy R, Tiwaria M, Donellib G, Tiwaria V. Strategies for combating bacterial biofilms: A focus on anti-biofilm agents and their mechanisms of action. Virulence. 2018;9(1):522–54. doi: 10.1080/21505594.2017.1313372.

[13] Arciola CR, Campoccia D, Montanaro L. Implant infections: adhesion, biofilm formation and immune evasion. Nature Rev Microb. 2018;16(7):397–409. doi: 10.1038/s41579-018-0019-y.

[14] Kumar A, Alam A, Rani M, Ehtesham NZ, Hasnain SE. Biofilms: survival and defense strategy for pathogens. Int J Med Microbiol. 2017;307(8):481–9. doi: 10.1016/j.ijmm.2017.09.016.

[15] McConoughey SJ, Howlin R, Granger JF. Biofilms in periprosthetic orthopedic infections. Future Microbiol. 2014;9:987–1007. doi: 10.2217/fmb.14.64.

[16] Kolmas J, Groszyk E, Kwiatkowska-Różycka D. Substituted hydroxyapatites with antibacterial properties. Biomed Res Int. 2014;2014(2):178123. doi: 10.1155/2014/178123.

[17] Lim PN, Chang L, Thian ES. Development of nanosized silver-substituted apatite for biomedical applications: a review.

Nanomedicine. 2015;11(6):1331–44. doi: 10.1016/j.nano.2015.03.016.
[18] Ciobanu CS, Iconaru SL, Chifiriuc MC, Costescu A, Coustumer PL, Predoi D. Synthesis and antimicrobial activity of silver-doped hydroxyapatite nanoparticles. Biomed Res Int. 2013;2013:916218. doi: 10.1155/2013/916218.
[19] Samani S, Hossainalipour SM, Tamizifar M, Rezaie HR. *In-vitro* antibacterial evaluation of sol-gel-derived Zn–, Ag–, and (Zn + Ag)-doped hydroxyapatite coatings against methicillin-resistant *S. aureus*. J Biomed Mater Res A. 2013;101(1):222–30. doi: 10.1002/jbm.a.34322.
[20] Shanmugam S, Gopal B. Copper substituted hydroxyapatite and fluorapatite: synthesis, characterization and antimicrobial properties. Ceram Int. 2014;40(10):15655–62. doi: 10.1016/j.ceramint.2014.07.086.
[21] Wang X, Ito A, Sogo Y, Li X, Oyane A. Zinc-containing apatite layers on external fixation rods promoting cell activity. Acta Biomater. 2010;6(3):962–8. doi: 10.1016/j.actbio.2009.08.038.
[22] Ofudje EA, Adeogun AI, Idowu MA, Kareem SO. Synthesis and characterization of Zn-doped hydroxyapatite: scaffold application, antibacterial and bioactivity studies. Heliyon. 2019;5(5):e01716. doi: 10.1016/j.heliyon.2019.e01716.
[23] Stanić V, Dimitrijević S, Antić-Stanković J, Mitrić M, Jokić B, Plećaš IB, et al. Synthesis, characterization and antimicrobial activity of copper and zinc-doped hydroxyapatite nanopowders. Appl Surf Sci. 2010;256(20):6083–9. doi: 10.1016/j.apsusc.2010.03.124.
[24] Thian ES, Konishi T, Kawanobe Y, Lim PN, Choong C, Ho B, et al. Zinc-substituted hydroxyapatite: a biomaterial with enhanced bioactivity and antibacterial properties. J Mat Sci Mater in Med. 2013;24(2):437–45. doi: 10.1007/s10856-012-4817-x.
[25] Udhayakumar G, Muthukumarasamy N, Velauthapillai D, Santhosh SB, Asokan V. Magnesium incorporated hydroxyapatite nanoparticles: preparation, characterization, antibacterial and larvicidal activity. Arab J Chem. 2016;11(5):645–54. doi: 10.1016/j.arabjc.2016.05.010.
[26] Alshemary AZ, Akram M, Goh YF, Tariq U, Butt FK, Abdolahid A. Synthesis, characterization, *in vitro* bioactivity and antimicrobial activity of magnesium and nickel doped silicate hydroxyapatite. Ceram Int. 2015;41:11886–98. doi: 10.1016/j.ceramint.2015.06.003.
[27] Predoi D, Iconaru SL, Predoi MV, Groza A, Gaiaschi S, Rokosz K, et al. Development of cerium-doped hydroxyapatite coatings with antimicrobial properties for biomedical applications. Coatings. 2020;10:516. doi: 10.3390/coatings10060516.
[28] Grenho L, Monteiro FJ, Ferraz MP. *In vitro* analysis of the antibacterial effect of nanohydroxyapatite–ZnO composites. J Biomed Mater Res Part A. 2014;102(10):3726–33. doi: 10.1002/jbm.a.35042.
[29] Silva-Holguín PN, Reyes-López SY. Synthesis of hydroxyapatite-Ag composite as antimicrobial agent. Dose-Response. 2020;2020(1):1–14. doi: 10.1177/1559325820951342.
[30] Rode TM, Rode TM, Langsrud S, Holck A, Moretro T. Different patterns of biofilm formation in *Staphylococcus aureus* under food-related stress conditions. Int J Food Microbiol. 2007;116(3):372–83. doi: 10.1016/j.ijfoodmicro.2007.02.017.
[31] Hiramatsu K, Katayama Y, Matsuo M, Sasaki T, Morimoto Y, Sekiguchi A, et al. Multi-drug-resistant *Staphylococcus aureus* and future chemotherapy. J Infect Chemother. 2014;20(10):593–601. doi: 10.1016/j.jiac.2014.08.001.
[32] Tolker-Nielsen T. *Pseudomonas aeruginosa* biofilm infections: from molecular biofilm biology to new treatment possibilities. APMIS. 2014;122:1–51. doi: 10.1111/apm.12335.
[33] Mas-Moruno C, Su B, Dalby MJ. Multifunctional coatings and nanotopographies: toward cell instructive and antibacterial implants. Adv Healthc Mater. 2019;8:1801103. doi: 10.1002/adhm.201801103.
[34] Parikh MS, Antony S. A comprehensive review of the diagnosis and management of prosthetic joint infections in the absence of positive cultures. J Infect Public Heal. 2016;9(5):545–56. doi: 10.1016/j.jiph.2015.12.001.
[35] Livitska O, Strutynska N, Zatovsky I, Nikolenko I, Slobodyanik N, Prylutskyy Y, et al. Copper(II), zinc(II) and copper(II)/zinc(II)-containing carbonate-substituted hydroxyapatite: synthesis, characterization and thermal behaviour. Mat-wiss u Werkstofftech. 2016;47:85–91. doi: 10.1002/mawe.201600460.
[36] Strutynska N, Zatovsky I, Slobodyanik N, Malyshenko A, Prylutskyy Yu, Prymak O, et al. Preparation, characterization, and thermal transformation of poorly crystalline sodium- and carbonate-substituted calcium phosphate. Eur J Inorg Chem. 2015;4:622–9. doi: 10.1002/ejic.201402761.
[37] Benito N, Franco M, Ribera A, Soriano A, Rodriguez-Pardo D, Sorlí L, et al. Time trends in the aetiology of prosthetic joint infections: a multicentre cohort study. Clin Microbiol Infect. 2016;22:e1–8. doi: 10.1016/j.cmi.2016.05.004.
[38] Javier A, Enrique E-G, Díaz B. Antimicrobial and antibiofilm activity of biopolymer-Ni, Zn nanoparticle biocomposites synthesized using R. Mucilaginosa UANL-001Lexopolysaccharide as a capping agent. Int J Nanomed. 2019;14:2557–71. doi: 10.2147/IJN.S196470.
[39] Seil JT, Webster TJ. Reduced *Staphylococcus aureus* proliferation and biofilm formation on zinc oxide nanoparticle PVC composite surfaces. Acta Biomater. 2011;7(6):2579–84. doi: 10.1016/j.actbio.2011.03.018.
[40] Gómez-Gómez B, Arregui L, Serrano S, Santos A, Pérez-Corona T, Madrid Y. Unravelling mechanisms of bacterial quorum sensing disruption by metal-based nanoparticles. Sci Total Environ. 2019;696:133869. doi: 10.1016/j.scitotenv.2019.133869.
[41] Yarawsky AE, Johns SL, Schuck P, Herr AB. The biofilm adhesion protein Aap from *Staphylococcus epidermidis* forms zinc-dependent amyloid fibers. J Biol Chem. 2020;295(14):4411–27. doi: 10.1074/jbc.RA119.010874.
[42] Soutourina O, Dubrac S, Poupel O, Msadek T, Martin-Verstraete I. The pleiotropic CymR regulator of staphylococcus aureus plays an important role in virulence and stress response. PLoS Pathog. 2010;6(5):e1000894. doi: 10.1371/journal.ppat.1000894.
[43] Livitska OV, Strutynska NYu, Vasyliuk OM, Grynyuk II, Prylutska SV, Slobodyanik NS. Synthesis, characterization and antimicrobial properties of chemically modified apatite-related calcium phosphates. Funct Mater. 2020;27(1):184–91. doi: 10.15407/fm27.01.184.

[44] Wang W, Li TL, Wong HM, Chu PK, Kao RYT, Wu S, et al. Development of novel implants with self-antibacterial performance through *in-situ* growth of 1D ZnO nanowire. Colloid Surf B Biointerfaces. 2016;141:623–33. doi: 10.1016/j.colsurfb.2016.02.036.

[45] Shimada T, Yasui T, Yonese A, Yanagida T, Kaji N, Kanai M, et al. Mechanical rupture-based antibacterial and cell-compatible ZnO/SiO_2 nanowire structures formed by bottom-up approaches. Micromachines. 2020;11:610. doi: 10.3390/mi11060610.